© 2014. Published by The Company of Biologists Ltd | Journal of Cell Science (2014) 127, 5066–5078 doi:10.1242/jcs.158840

RESEARCH ARTICLE

Phosphorylation of threonine 3 on histone H3 by haspin kinase is required for meiosis I in mouse oocytes

Alexandra L. Nguyen, Amanda S. Gentilello, Ahmed Z. Balboula*, Vibha Shrivastava, Jacob Ohring and Karen Schindler‡

ABSTRACT

Meiosis I (MI), the division that generates haploids, is prone to errors that lead to aneuploidy in females. Haspin is a kinase that phosphorylates histone H3 on threonine 3, thereby recruiting Aurora kinase B (AURKB) and the chromosomal passenger complex (CPC) to kinetochores to regulate mitosis. Haspin and AURKC, an AURKB homolog, are enriched in germ cells, yet their significance in regulating MI is not fully understood. Using inhibitors and overexpression approaches, we show a role for haspin during MI in mouse oocytes. Haspin-perturbed oocytes display abnormalities in chromosome morphology and alignment, improper kinetochore–microtubule attachments at metaphase I and aneuploidy at metaphase II. Unlike in mitosis, kinetochore localization remained intact, whereas the distribution of the CPC along chromosomes was absent. The meiotic defects following haspin inhibition were similar to those observed in oocytes where AURKC was inhibited, suggesting that the correction of microtubule attachments during MI requires AURKC along chromosome arms rather than at kinetochores. Our data implicate haspin as a regulator of the CPC and chromosome segregation during MI, while highlighting important differences in how chromosome segregation is regulated between MI and mitosis.

KEY WORDS: Haspin kinase, Aurora kinase, Histone phosphorylation, Meiosis I, Meiotic maturation, Oocyte

INTRODUCTION

Meiosis, the cellular process that generates haploid gametes from diploid precursors, is prone to errors in females (Hunt and Hassold, 2002). A significant percentage of mistakes in segregating homologs arise during meiosis I (MI). These errors are the leading genetic cause of miscarriage in women. Therefore, determining the molecular underpinnings that control this unique chromosome segregation is of great interest.

Haspin (also known as GSG2) is an atypical serine/threonine protein kinase that is conserved from yeast to humans (Higgins, 2003). Haspin mRNA was first discovered in mouse spermatocytes in a subtracted cDNA screen to discover meiosis-specific genes (Tanaka et al., 1999). Although it is highly expressed in male gametes, haspin mRNA is also expressed in somatic cells, albeit to a lesser extent. However, it is not known whether haspin is required for meiosis in oocytes. To date, the only known haspin substrates are threonine 3 of histone H3 (H3T3), serine 137 of macroH2A and threonine 57 of CENP-T (Maiolica et al., 2014). Knockdown or inhibition of haspin in mitotically dividing tissue culture cell lines reveal that phosphorylation of H3T3 is essential for the alignment of chromosomes at the metaphase plate (Dai and Higgins, 2005; Dai et al., 2005), regulation of chromosome cohesion (Dai et al., 2009) and establishing a bipolar spindle (Dai et al., 2009). In mitotic metaphase, phosphorylation of H3T3 is restricted to kinetochores, and this mark signals recruitment of the chromosomal passenger complex (CPC) (Dai et al., 2005; Wang et al., 2010; Yamagishi et al., 2010). The CPC then navigates the cell through the metaphase–anaphase transition by correcting improper kinetochore–microtubule attachments, thereby controlling the alignment of chromosomes at the metaphase plate (Carmena et al., 2012; Kelly and Funabiki, 2009). During anaphase, H3T3 is dephosphorylated and the CPC moves to the spindle midzone where it regulates cytokinesis (Qian et al., 2011). Therefore, phosphorylation of H3T3 by haspin is a mark that dictates localized CPC activity essential for the mitotic cell cycle.

Aurora B kinase (AURKB) is the catalytic subunit of the CPC in mitosis. Meiotic cells contain an AURKB homolog called Aurora C kinase (AURKC), which also functions within the CPC (Li et al., 2004; Sasai et al., 2004; Sharif et al., 2010; Tseng et al., 1998). In mitotic cells where AURKB has been depleted, ectopic expression of AURKC can rescue the cytokinesis defects (Sasai et al., 2004). We previously demonstrated that oocytes express both AURKB and AURKC (Balboula and Schindler, 2014; Shuda et al., 2009), and that AURKB can functionally compensate for loss of AURKC in mouse oocytes (Schindler et al., 2012). However, AURKC localizes to kinetochores and the interchromatid axis (ICA) during metaphase I (Met I), whereas AURKB localizes to the spindle, supporting the model that they have some non-overlapping functions during MI in wild-type oocytes. Consistent with its localization to chromosomes, we found that AURKC is uniquely required to correct improper kinetochore–microtubule attachments to generate euploid metaphase II (Met II) eggs. AURKC localization to chromosomes is governed by its own catalytic activity and by histone deacetylation (Balboula and Schindler, 2014; Balboula et al., 2014); however, it is not known how AURKC loading is specifically regulated.

Here, we demonstrate that mouse oocytes contain haspin kinase activity, and that haspin is required for proper completion of MI by maintaining bivalent chromosome structure through regulation of condensin, and not cohesin. To our surprise, perturbation of haspin activity did not affect kinetochore-localized AURKC-CPC but specifically ablated ICA-localized AURKC-CPC. However, we

Department of Genetics, Rutgers, The State University of New Jersey, Piscataway, NJ 08854, USA.
*Present address: Theriogenology Department, Faculty of Veterinary Medicine, Mansoura University, Mansoura 35516, Egypt.

‡Author for correspondence (schindler@biology.rutgers.edu)

Received 27 June 2014; Accepted 2 October 2014

Journal of Cell Science

Journal of Cell Science (2014) 127, 5066–5078 doi:10.1242/jcs.158840

still observed improper kinetochore–microtubule attachments and subsequent aneuploidy, consistent with loss of AURKC activity. These data suggest that the correction of these attachments during Met I requires AURKC activity along the ICA, and they indicate that haspin activity regulates meiotic AURKC-CPC localization differently than it does AURKB-CPC in mitosis.

RESULTS

Haspin protein kinase expression, activity and localization during meiosis in mouse oocytes

Although haspin was identified as a germ-cell-specific gene expressed in mouse testes (Tanaka et al., 1999) and noted as a key regulator of the mitotic cell cycle in somatic cells (Dai and Higgins, 2005; Dai et al., 2009; Dai et al., 2006; Dai et al., 2005; De Antoni et al., 2012; Huertas et al., 2012; Wang et al., 2012; Yamagishi et al., 2010), its role in meiosis and specifically in oocyte meiotic maturation is still not known. To first determine whether an H3T3 kinase exists in mouse oocytes, we performed immunocytochemistry using an antibody that recognizes phosphorylated H3T3 (H3pT3) on *in-vitro*-matured oocytes fixed at different stages of meiotic maturation. We found that H3T3 was phosphorylated during metaphase of MI (Met I) and metaphase of MII (Met II) (Fig. 1A). Phosphorylation persisted in anaphase I (Ana I), but was absent during telophase I (Telo I). During Met I, we found this histone mark not only at centromeres but also along the ICA. Notably, H3T3 phosphorylation along the ICA is meiosis specific, because its phosphorylation is restricted to centromeres in mitosis (Dai et al., 2006; Markaki et al., 2009). These data suggest that oocytes contain haspin, and demonstrate that the localization pattern of H3pT3 differs in Met I from the pattern observed during metaphase of mitosis.

To determine whether haspin mRNA is expressed in oocytes, we performed quantitative RT-PCR on cDNA libraries generated from mouse oocytes and preimplantation embryos. The data indicate that haspin is a maternally expressed gene that persists during meiosis and in one-cell embryos prior to its destruction (Fig. 1B). Compared with maternal expression levels, zygotic expression is not as abundant (<30%), consistent with observed low expression levels in somatic cells (Tanaka et al., 1999). Therefore, oocytes undergoing meiotic maturation contain haspin mRNA.

Next, we wanted to determine whether haspin protein was expressed in oocytes. We found that commercially available antibodies indicated to react with endogenous haspin were not specific in our system (data not shown). To correlate H3pT3 with localization of haspin, we expressed *Gfp*-tagged haspin cRNA in mouse oocytes. GFP–haspin colocalized with chromatin and H3pT3 during all meiotic stages assessed (Fig. 1C,D). Notably, the levels of H3pT3 increased twofold with the addition of exogenous haspin, further supporting that haspin is the H3T3 kinase in oocytes (Fig. 1D). At Met I, we detected haspin at centromeres and at sister chromatid axes (Fig. 1C). In conducting these experiments, we found that, starting at Met I, GFP–haspin also localized to a discrete region of the oocyte cortex that is in close proximity to the chromatin and spindle (Fig. 1E). Actin is restricted to this cortical region, giving this subcellular locale the name ‘actin cap’. To determine whether haspin colocalizes with the actin cap, we detected actin with TRITC-tagged phalloidin in oocytes expressing GFP–haspin. As expected, ectopically expressed haspin colocalized with the actin cap (Fig. 1E). This localization was disrupted upon treatment with latrunculin A, an actin depolymerizing agent (Fig. 1F). Haspin is implicated in regulating asymmetric cell divisions in budding yeast (Panigada et al., 2013) and in *Arabidopsis thaliana* embryos (Ashtiyani et al., 2011). Because cytokinesis during MI in oocytes is also asymmetric, these data are consistent with haspin having at least one additional substrate that is perhaps specific to asymmetrically dividing cells. Taken together, these data suggest that haspin phosphorylates H3T3 in a MI-specific pattern along the ICA.

Haspin activity is required for meiotic progression

Inhibition of haspin in somatic cells causes a host of phenotypic consequences, including prolonged length of time to anaphase onset, chromosome misalignment and lagging chromosomes (Dai and Higgins, 2005; Dai et al., 2006; Dai et al., 2005; De Antoni et al., 2012; Huertas et al., 2012; Markaki et al., 2009; Wang et al., 2012; Yamagishi et al., 2010). To determine whether haspin activity is required for oocyte meiotic maturation, we matured oocytes in 5-iodotubercidin (5-Itu), a small-molecule inhibitor with high specificity for haspin (De Antoni et al., 2012; Wang et al., 2012). We first confirmed that 5-Itu inhibited haspin, by detecting H3pT3 using immunocytochemistry. Compared with control oocytes incubated in vehicle (100% ethanol), H3pT3 signals were reduced by 90% Met I in oocytes incubated in 100 nM of 5-Itu and were nearly absent when oocytes were incubated in 500 nM of 5-Itu (Fig. 2A). Overexpression of haspin rescued the loss of H3pT3 in 5-Itu-treated oocytes (Fig. 2B). This rescue depended on the catalytic activity of haspin, because a mutant in the ATP-binding pocket (K466R) could not rescue loss of H3pT3, further supporting that haspin is the H3T3 kinase in oocytes. Within 1 h after adding the drug, H3pT3 signals diminished and did not return (supplementary material Fig. S1). We observed similar results when oocytes were treated with the same doses of CHR-6494 (CHR) (Huertas et al., 2012), another small-molecule inhibitor of haspin (supplementary material Fig. S2A). These data indicate that, similar to mitotic cycling cells (De Antoni et al., 2012; Huertas et al., 2012; Wang et al., 2012), haspin activity can be inhibited in oocytes by the addition of small-molecule inhibitors to *in vitro* culture medium. Moreover, we note that the dose required to inhibit haspin in oocytes and in our subsequent experiments was approximately tenfold less than the 5-Itu doses used to inhibit haspin in mitotic cells (De Antoni et al., 2012; Wang et al., 2012).

Oocytes remain arrested at the prophase of MI until they are removed from follicles and resume meiosis. The first morphological event during meiotic maturation is nuclear envelope breakdown (NEBD), which occurs when oocytes resume meiosis and enter Met I. Control oocytes underwent NEBD between 1.5 and 2 h after induction of meiotic maturation (Fig. 2C). We observed slightly reduced meiotic-resumption kinetics in 20% of oocytes compared with controls when oocytes were matured in the presence of 100 nM 5-Itu. By contrast, when we increased the concentration of 5-Itu to 500 nM, all oocytes took 1 h longer to resume meiosis and 40% of oocytes failed to resume even after 5 h of incubation. Perturbations of meiotic-resumption kinetics were not specific to 5-Itu because CHR treatment also caused delays (supplementary material Fig. S2B), and these delays are consistent with a reported delay in the G2-M transition in HeLa cells depleted of haspin (Dai et al., 2006).

To determine the consequences of haspin inhibition for meiotic maturation, we fixed the treated cells at 16 h – the time at which controls extruded a polar body and arrested at Met II (Fig. 2D) – and performed immunocytochemistry to determine the final

Journal of Cell Science (2014) 127, 5066–5078 doi:10.1242/jcs.158840

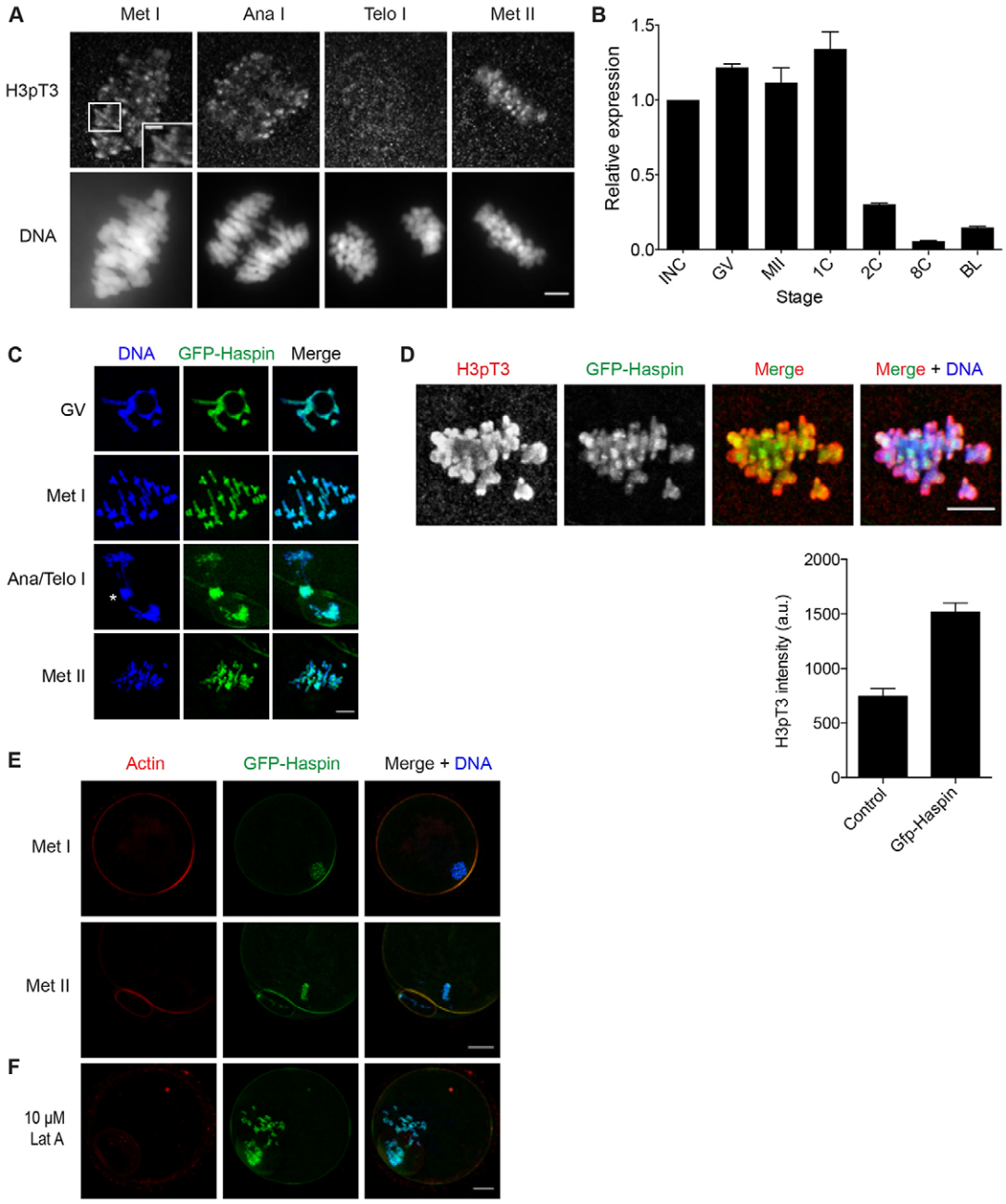

Fig. 1. Mouse oocytes contain active haspin protein kinase. (A) Germinal-vesicle-intact oocytes were isolated and matured *in vitro* to the indicated stages prior to fixation and detection of phosphorylated threonine 3 on histone 3 (H3pT3) and DNA. Shown are optical slices obtained by confocal microscopy from a representative experiment. The experiment was repeated three times with ≥15 oocytes per stage. (B) Relative mRNA levels of haspin in oocytes and preimplantation embryos. Expression levels were determined by quantitative RT-PCR and were normalized against exogenous *Gfp*. Data are shown as the mean±s.e.m. (three independent experiments). (C–F) Germinal-vesicle-intact oocytes were isolated, microinjected with Gfp-haspin cRNA and matured *in vitro* to the indicated stages prior to fixation and processing to detect GFP–haspin (green), DNA (blue), H3pT3 (red) (D) or actin (red) (E,F). Asterisk, chromosomes in an anaphase bridge. (F) Met II eggs were incubated in 10 μM of latrunculin A (Lat A) for 10 min prior to fixation. Shown are representative *Z*-projections obtained using confocal microscopy. Quantification of H3T3 phosphorylation levels are also shown, as the mean±s.e.m. a.u., arbitrary units. The experiments were conducted at least twice, with 15 oocytes in each group. INC, incompetent oocyte; 1C, 1-cell embryo; 2C, 2-cell embryo; 8C, 8-cell embryo; BL, blastocyst; GV, germinal vesicle; Met I, metaphase I; Ana I, anaphase I; Telo I, telophase I, MII or Met II, metaphase II. Scale bars: 10 μm (A,C–F), 2 μm (inset in A).

meiotic stage reached. At the lower dose, ~80% of oocytes reached Met II (Fig. 2D). Of those oocytes that failed to reach Met II, 10% were at Met I and 5% were in Telo I. When treated with 500 nM 5-Itu, only ~60% of oocytes reached Met II. About the same percentage of oocytes were at Met I as observed in samples treated with the lower dose, but more failed to resume meiosis. These results were similar to those obtained when oocytes were matured in the presence of CHR (Fig. 2E). Furthermore, we occasionally observed eggs with polar bodies that contained DNA collapsed into a ball-like structure (described as collapsed), which sometimes reformed a nucleolus as if the oocyte had entered interphase (described as interphase). We

Journal of Cell Science (2014) 127, 5066–5078 doi:10.1242/jcs.158840

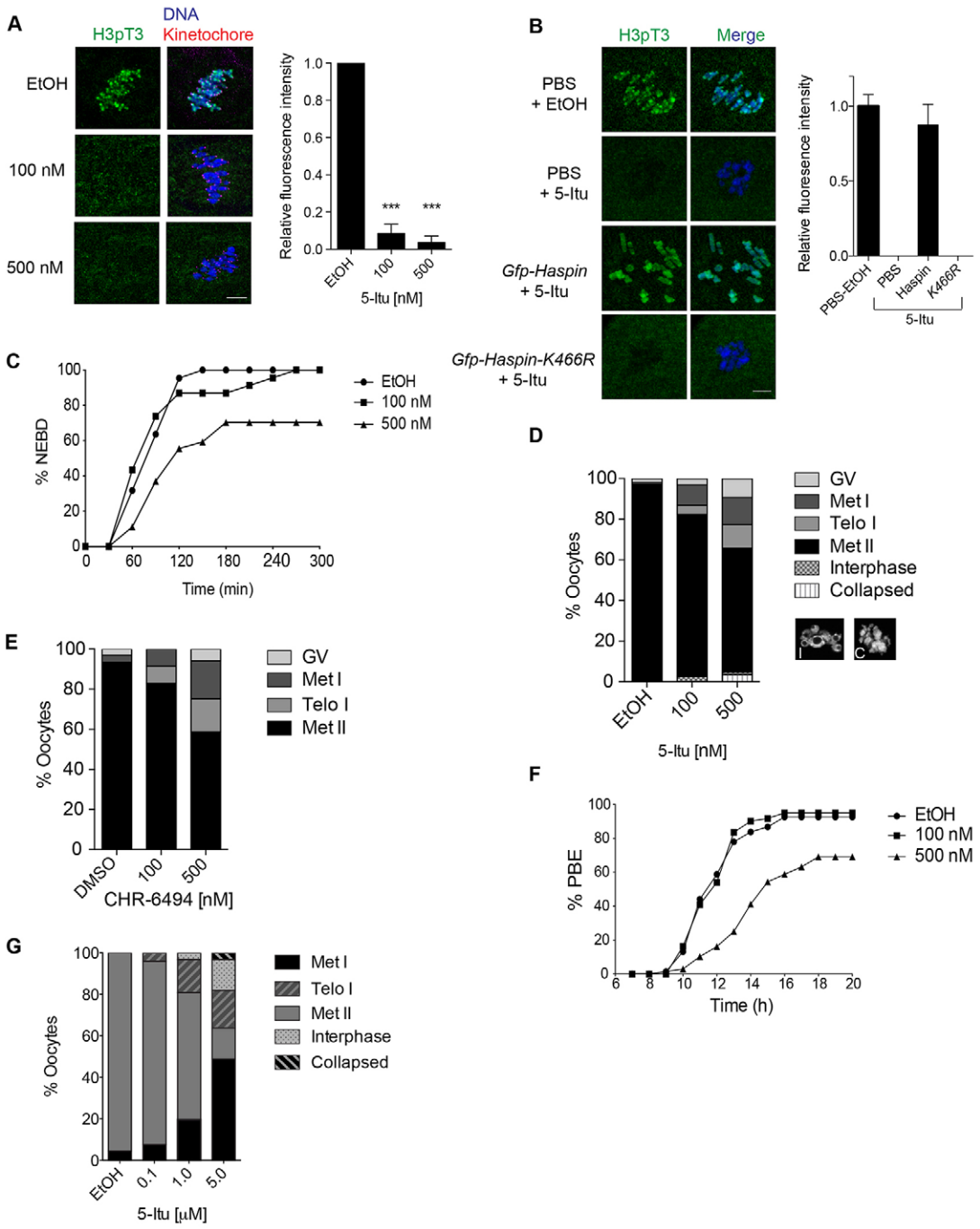

Fig. 2. Inhibition of haspin perturbs MI. Prophase-I-arrested oocytes were isolated and matured *in vitro* in the presence of the indicated concentration of 5-iodotubercidin (5-Itu) or CHR-6494 (CHR) prior to analysis. The drugs were added to culture medium containing oocytes with an intact nuclear envelope in A–F or oocytes that underwent nuclear envelope breakdown (NEBD) in G. (A,B) Oocytes were matured to Met I (7 h) prior to fixation and detection of phosphorylated threonine 3 on histone 3 (H3pT3) (green), kinetochores [(A) CREST anti-serum] (red) and DNA (blue) in the presence of 5-Itu. Shown are representative *Z*-projections obtained by confocal microscopy from one experiment. Quantification of the H3pT3 signals are shown to the right of each image panel. (B) The indicated material was microinjected 1 h after the addition of ethanol (EtOH) or 500 nM of 5-Itu. For A,B, data are shown as the mean±s.e.m.; ***$P<0.001$ (one-way ANOVA). Scale bars: 10 μm. (C) The timing of NEBD as determined by live-cell imaging when oocytes were matured in the indicated dose of 5-Itu. Images were captured every 30 min. (D,E,G) Analysis of the meiotic stage reached after maturation in the indicated drug for 16 h, as determined by confocal microscopy. Examples of interphase ('I') and collapsed ('C') oocytes are shown below the key. (F) Timing of polar body extrusion (PBE) as determined by live-cell imaging when oocytes were matured in the indicated dose of 5-Itu. The data were corrected for delay in NEBD prior to analysis. These experiments were repeated three times with ≥15 oocytes per group. GV, germinal vesicle; Met I, metaphase I; Ana I, anaphase I; Telo I, telophase I, Met II, metaphase II.

speculate that these rare phenotypes arose owing to failed attempt to undergo cytokinesis. We also used live-cell imaging to more closely examine the kinetics with which the oocytes were progressing through MI. Completion of MI was defined by extrusion of the polar body. After correcting for the delay in meiotic resumption, control oocytes and those treated with

Journal of Cell Science (2014) 127, 5066–5078 doi:10.1242/jcs.158840

100 nM 5-Itu extruded polar bodies with similar kinetics, starting at ~10 h after induction of meiotic maturation (Fig. 2F; supplementary material Movies 1, 2). Despite correcting for the NEBD delay (Fig. 2C), oocytes treated with 500 nM 5-Itu exhibited a delay in completing MI by ~2 h compared with controls (supplementary material Movie 3). Similar to the results in Fig. 2D, only 60% of these oocytes extruded polar bodies in a timely manner. Therefore, similar to a delay of anaphase onset in mitosis, haspin activity is required for timely completion of MI in mouse oocytes.

To confirm that failure to progress to Met II was not a consequence of perturbing NEBD, we allowed oocytes to complete NEBD prior to addition of the inhibitor. Similar to our observations presented in Fig. 2D, inhibition of haspin later in meiotic maturation still compromised completion of MI, but required a roughly twofold higher dose than when treating oocytes prior to NEBD, reflecting either the later timing of haspin inhibition (Fig. 2G) or the apparent increase in haspin activity after NEBD (supplementary material Fig. S1). Starting at 1 µM, more oocytes were still delayed in Met I and Telo I than in controls or 100 µM 5-Itu-treated oocytes. Therefore, the deficiency in completing meiotic maturation was not a consequence of impeding meiotic resumption when haspin was inhibited. Regardless of the time of drug addition with respect to meiotic stage or the drug that we used to inhibit haspin, we observed nearly identical phenotypic consequences – delays in NEBD and polar body extrusion, and collapsed DNA structures that eventually re-enter an interphase-like state.

Alteration of haspin activity perturbs chromosome morphology by delocalizing condensin

During the meiotic maturation experiments, we observed several abnormalities in the oocytes delayed in Met I when haspin activity was inhibited. To more closely assess these abnormalities, we matured control and haspin-inhibited oocytes to Met I prior to fixation and detection of spindles and chromosomes. Compared with controls and oocytes matured in 100 nM 5-Itu, oocytes matured in 500 nM 5-Itu frequently displayed abnormal chromosomal morphology. Control and 100 nM 5-Itu-treated oocytes contained clearly identifiable bivalent chromosomes nearly 95% of the time (Fig. 3A). However, when haspin was inhibited with the higher dose of 5-Itu, we observed fewer Met I oocytes with obvious bivalent chromosome structures (~60%) and more that contained either chromosomes with regions that appeared extended and overly 'pointy' at the ends (~5%) or chromosomes that were rounded and unusually compact (~35%). This phenotype was rescued when we overexpressed haspin in 5-Itu-treated oocytes, because we were able to detect normal-shaped bivalents in 75% of the oocytes. Furthermore, this rescue depended upon the catalytic activity of haspin (Fig. 3B). By contrast, and compared to control-injected oocytes, when we overexpressed haspin, we observed the opposite phenotype – the chromosomes appeared elongated as if they were unraveling when matured to Met II (Fig. 3C,D). Furthermore, oocytes in Ana I always contained chromosomes that formed anaphase bridges between segregating chromosomes (Fig. 1C; supplementary material Movies 4, 5). We note that we only observed abnormal morphology in the overexpression experiments after exit from Met I. To compare the chromosome morphology between 5-Itu-treated and haspin-overexpressing eggs at Met II, we performed chromosome spreads and measured the area of each sister chromatid (Fig. 3D,E). Both perturbations reduced the area of the chromatid (Fig. 3E). In 5-Itu-treated oocytes, the chromatids are smaller in area because they are more rounded, whereas in the haspin-overexpressing oocytes the area is smaller because they are thinner (Fig. 3D). Therefore, perturbation of haspin activity alters chromosome morphology during MI.

These chromosome morphology phenotypes are identical to the phenotypes observed when subunits of condensin were altered in mouse oocytes (Lee et al., 2011). Condensin is a multi-protein complex that regulates chromosome compaction in mitosis and meiosis. Cells contain two complexes, condensin I and condensin II. SMC2 is a protein that is common to both complexes. Similar to haspin, SMC2 is present at centromeres and at sister chromatid axes in mouse oocytes at Met I (Lee et al., 2011). To determine whether the abnormal chromosome morphology could be correlated with loss of localized condensin, we performed immunocytochemistry on oocytes that were matured to Met I in the presence of the haspin inhibitor. Control oocytes contained SMC2, as reported previously (Fig. 3F,G). By contrast, inhibition of haspin decreased detectable SMC2 by 20% following treatment with 100 nM 5-Itu and by 60% after treatment with 500 nM 5-Itu (Fig. 3G). Consistent with these data, in oocytes where we overexpressed haspin, we found a twofold increase in the amount of SMC2 on Met I chromosomes (Fig. 3H,I). In mitosis, haspin inhibition causes loss of cohesin at centromeres (Dai et al., 2006). We also assessed sister chromatid cohesin in 5-Itu-treated oocytes by conducting immunocytochemistry of Met I oocytes. Detection of the meiosis-specific REC8 cohesin subunit revealed that, in Met I, inhibition of haspin did not perturb cohesin (Fig. 4A,B). These data are further supported by the presence of SGOL2 at centromeres, indicating that sister chromatid cohesion is still intact and protected from premature proteolysis (Fig. 4C) Furthermore, we did not detect changes in REC8 localization or levels when haspin was overexpressed (Fig. 4D,E). Therefore, these data suggest that haspin regulates the loading of condensin to meiotic chromosomes and does not regulate the removal of cohesin.

Alteration of H3pT3 levels prevents AURKC-CPC from localizing to MI ICA

In mitosis, phosphorylation of H3T3 recruits AURKB-CPC to centromeres to regulate chromosome alignment and kinetochore–microtubule attachment (Dai and Higgins, 2005; Dai et al., 2006; Dai et al., 2005; De Antoni et al., 2012; Wang et al., 2010; Wang et al., 2012; Yamagishi et al., 2010). To determine whether AURKC-CPC is regulated in the same manner, we detected endogenous AURKC by immunocytochemistry in oocytes matured in 5-Itu to Met I. In 100 nM of 5-Itu, 40% of oocytes still contained AURKC at centromeres and along the ICA (Fig. 5A,B). To our surprise, although oocytes lost H3pT3 both at centromeres and the ICA in 500 nM 5-Itu (Fig. 2A,B), Met I oocytes only lost AURKC along the ICA (Fig. 5A,B). To quantify the presence and amount of AURKC at centromeres, we plotted the signal intensities along individual chromosomes in each oocyte using CREST to mark the sister kinetochore pairs as the start and end points (Fig. 5C). These analyses confirmed our qualitative assessment that AURKC signal was reduced along the ICA compared with that of controls, but not at kinetochores. We found identical results when either 5-Itu or CHR was added to culture medium after oocytes completed NEBD (supplementary material Fig. S3A–D). Overexpression of AURKC in 5-Itu-treated oocytes did not rescue the ICA localization defect (data not shown). Therefore, H3pT3 is a prerequisite for driving

Journal of Cell Science (2014) 127, 5066–5078 doi:10.1242/jcs.158840

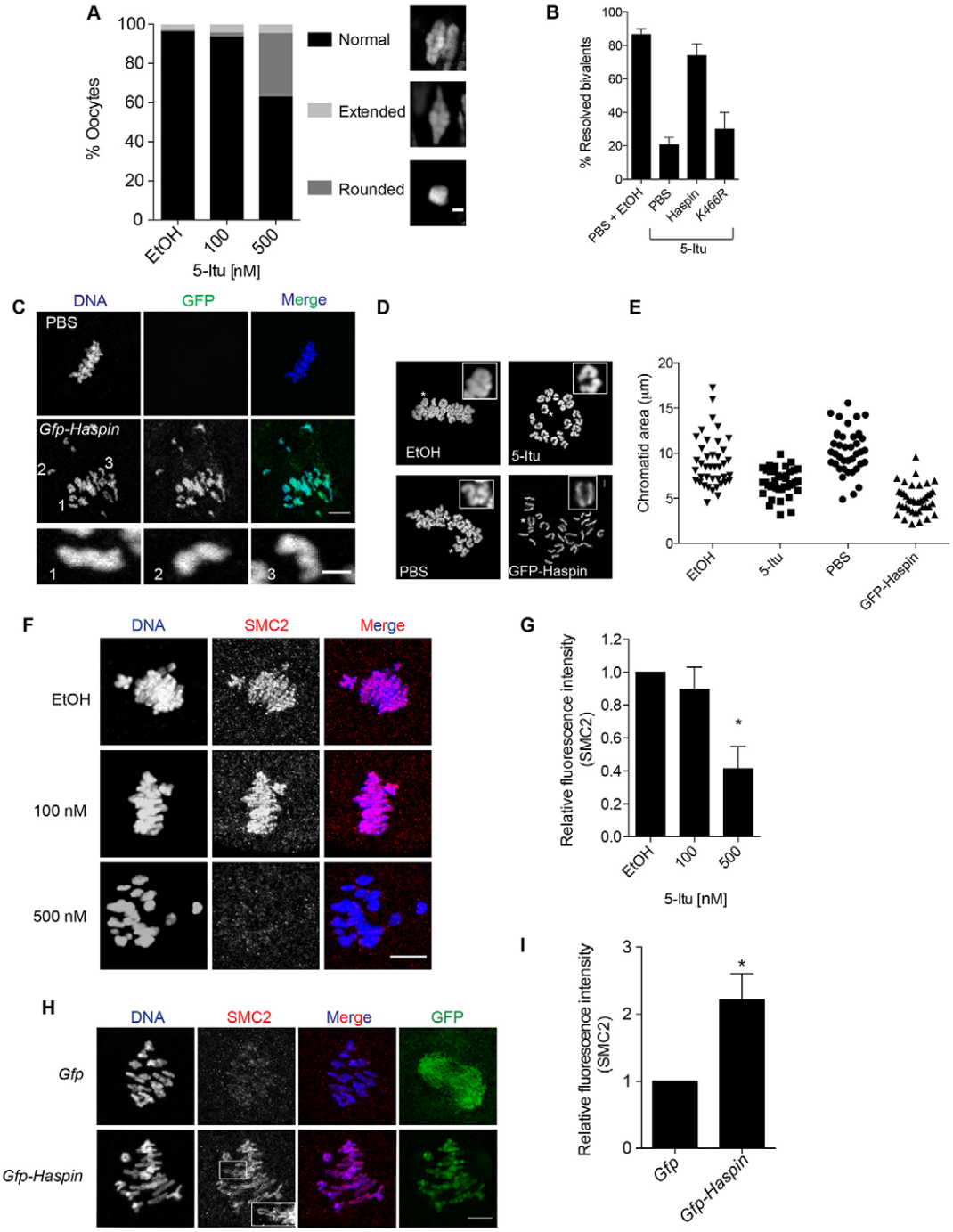

Fig. 3. Perturbation of haspin alters Met I chromosome morphology. (A,B,F,G) Prophase-I-arrested oocytes were isolated and matured *in vitro* to Met I [7 h (control) and 9 h (5-Itu)] in the presence of the indicated concentration of 5-iodotubercidin (5-Itu). (B) Prior to maturation, oocytes were microinjected with PBS, GFP–haspin or GFP–haspin-K466R. The 5-Itu dose was 500 nM. Resolved bivalents were equivalent to 'normal' in panel A. (C,H,I) Prophase-I-arrested oocytes were isolated, microinjected with the indicated cRNA (green) and matured *in vitro* to Met II (16 h) (C) or Met I (7 h) (H,I) prior to analysis of chromosome morphology by DAPI staining (C) or SMC2 localization (red, H) and abundance (I). (D) Oocytes were matured in ethanol (EtOH) or 500 nM 5-Itu, or microinjected with PBS or GFP–haspin before maturation to Met II (18 h) prior to lysis and spreading of chromosomes. (E) Area measurements were taken of each sister chromatids using the freehand line tool in ImageJ. Each point is the area of a single chromatid from the eggs in D. DNA was detected by DAPI staining. In C,D, the number labels and asterisks correspond to the magnified image panels demonstrating the morphology phenotypes. (F,H) SMC2 (red) and DNA (blue) were detected by immunocytochemistry. Shown are representative *Z*-projections obtained by confocal microscopy. In F,H, the laser power was set so that the brightest group was not saturated. These experiments were repeated at least three times with a mean of 15 oocytes per group. Data are expressed as the mean±s.e.m.; **P*<0.05 (one-way ANOVA, G; Student's *t*-test, I). Scale bars: 10 μm.

Journal of Cell Science (2014) 127, 5066–5078 doi:10.1242/jcs.158840

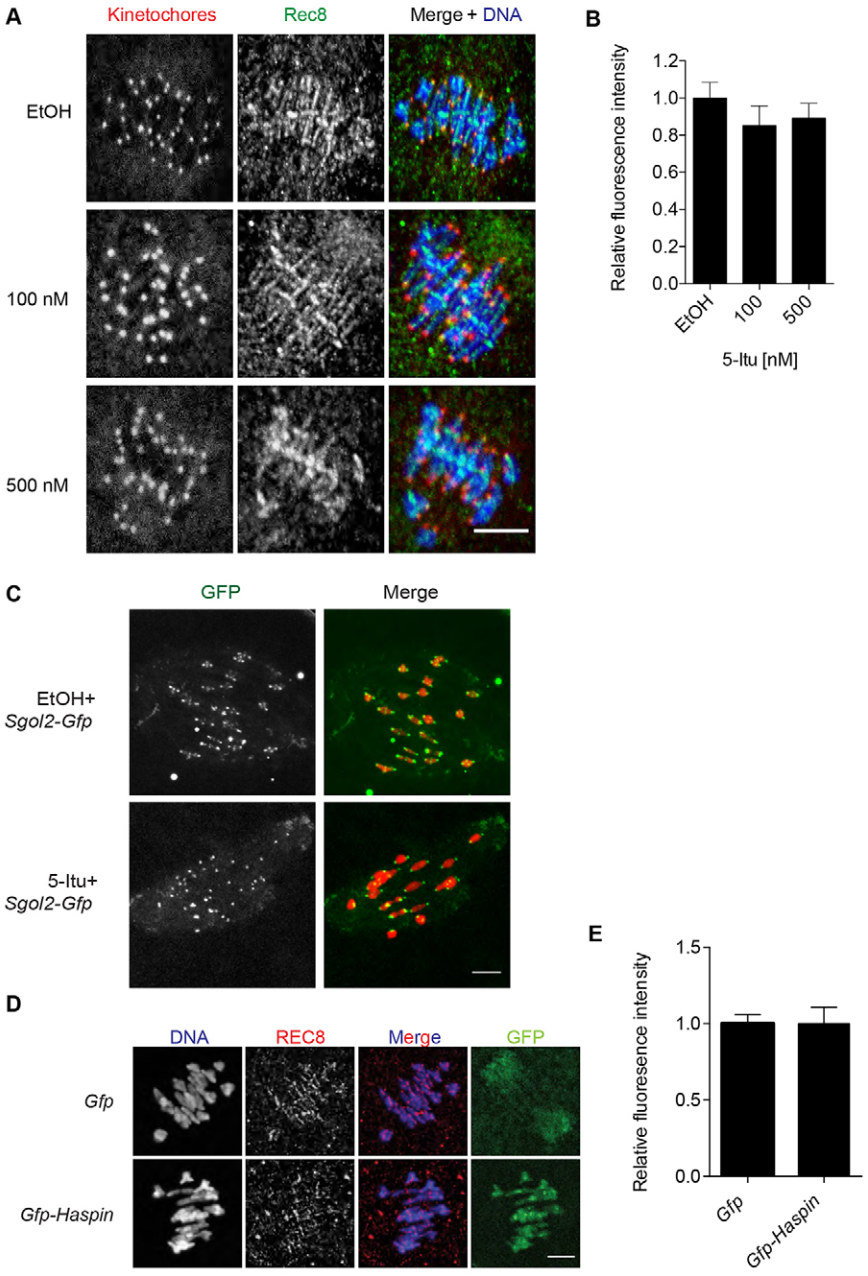

Fig. 4. Perturbation of haspin does not affect sister chromatid cohesion at Met I. (A,B) Germinal-vesicle-intact oocytes were isolated and matured *in vitro* to Met I (7 h) in the presence of the indicated concentrations of 5-Itu prior to fixation. Oocytes were stained for REC8 (green), kinetochores (CREST anti-sera, red) and DNA (blue). (C–E) Germinal-vesicle-intact oocytes were isolated, microinjected with the indicated cRNA and matured *in vitro* to Met I (7 h) prior to fixation. In C, ethanol (EtOH) or 5-Itu was added to the maturation medium. Samples were stained for REC8 (red) and DNA (red in C, blue in D). Shown are representative *Z*-projections obtained by confocal microscopy from the same experiment. Scale bars: 10 μm.
(B,E) Quantification of the REC8 signal along chromosomes. Data show the mean±s.e.m. These experiments were repeated at least twice with 10–15 oocytes per group. The data were not statistically significant [one-way ANOVA (B) or Student's *t*-test (E)].

localization of AURKC to the ICA but not to kinetochores during Met I.

To confirm that the CPC, and not just AURKC, is delocalized, we also detected the localization of survivin (also known as BIRC5) in 5-Itu-treated oocytes. In mitosis, survivin detects the H3pT3 mark and is responsible for docking the complex at kinetochores (Kelly et al., 2010; Niedzialkowska et al., 2012). Similar to AURKC, we observed loss of survivin along the ICA, but retention at kinetochores (Fig. 5D–F). Similar results were obtained when 5-Itu was administered after meiotic resumption (supplementary material Fig. S3E,F). This perturbed localization pattern of survivin was more severe in the 100 nM group than that of AURKC. However, the antibody that recognizes survivin is not as robust as the AURKC-specific antibody, and the differences might reflect this. Alternatively, some AURKC might localize to the ICA independent of the CPC. Regardless, ICA-localized CPC is perturbed when haspin is inhibited.

AURKB and AURKC phosphorylate a component of the CPC, called INCENP. To assess localized activity of AURKC, we detected the AURKC-phosphorylated form of INCENP (pINCENP) by immunocytochemistry. Similar to the results with AURKC, we observed a loss of pINCENP along the ICA beginning in the low dose of 5-Itu, and complete absence of pINCENP from the ICA in the high dose (Fig. 5G–I). Similar results were obtained when 5-Itu was administered after meiotic resumption (supplementary material Fig. S3G,H). Taken together, haspin activity is required to localize AURKC-CPC to the ICA but not to kinetochores during Met I.

We also conducted an experiment to drive excess AURKC-CPC to Met I chromosomes by overexpressing GFP–haspin. Although H3pT3 greatly increased all over the chromosomes

Journal of Cell Science (2014) 127, 5066–5078 doi:10.1242/jcs.158840

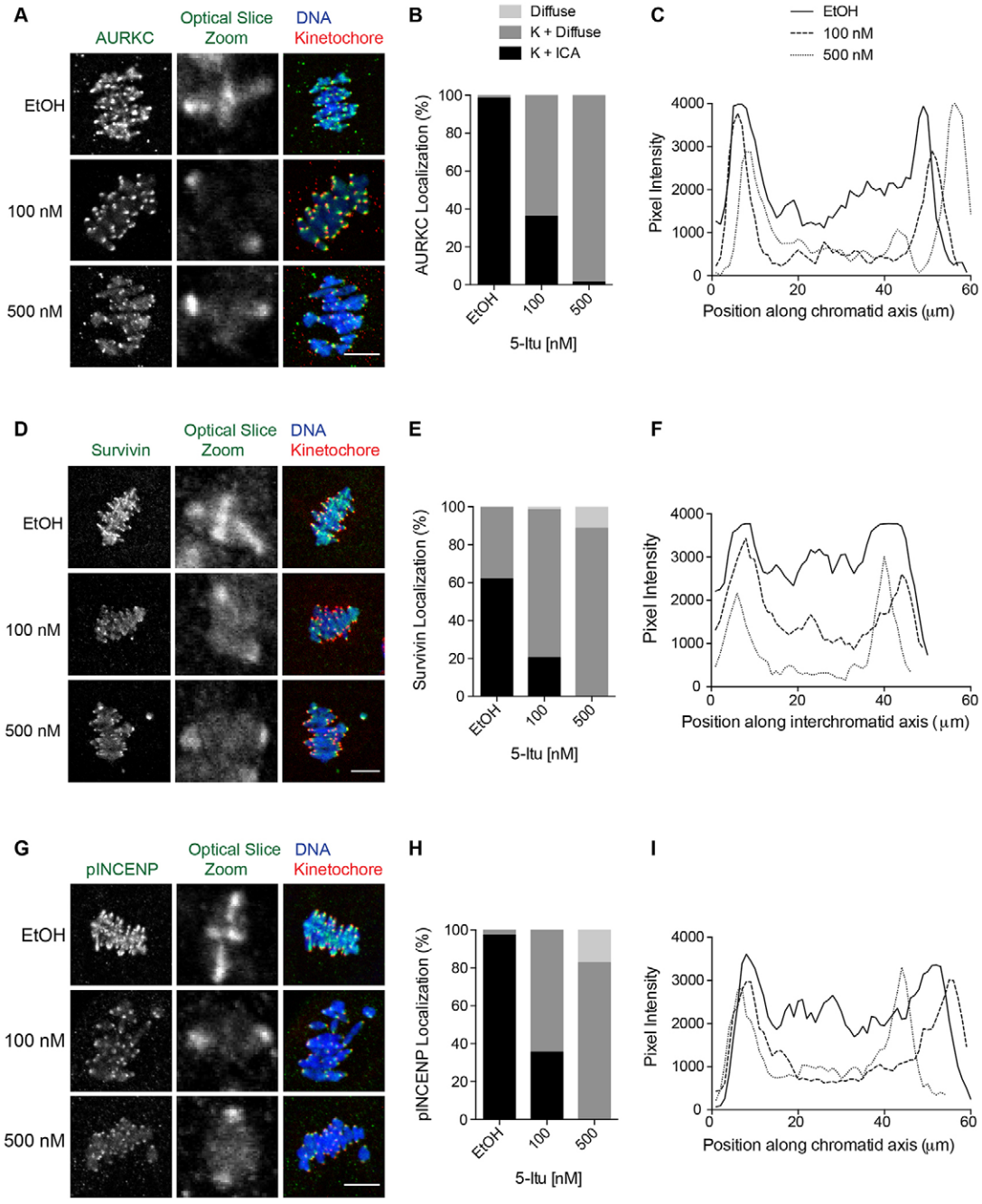

Fig. 5. Inhibition of haspin perturbs AURKC-CPC ICA localization. Prophase-I-arrested oocytes were isolated and matured *in vitro* to Met I (7 h for control, 9 h for 5-Itu) in the presence of the indicated concentrations of 5-iodotubercidin (5-Itu). (A,D,G) The indicated CPC subunits (green in merge) were detected by immunocytochemistry and shown are representative images. The 'zoom' panels highlight the presence of the CPC subunit remaining at the kinetochore (CREST antisera; red in merge) but diffusely localized along the ICA. The zoomed images show a selected chromosome from an optical slice before *Z*-projection. Scale bars: 10 μm. (B,E,H) Quantification of CPC subunit localization. K+diffuse, kinetochore and diffuse signal on interchromatid axis; K+ICA, kinetochore and interchromatid axis; diffuse, no kinetochore or interchromatid axis localization using a qualitative method. (C,F,I) Examples of quantitative assessment of the chromosome image in the zoom, using the 'plot profiles' function in ImageJ. The analyses show CPC subunit localization on chromosomes, following the use of CREST antisera to mark the kinetochores. These experiments were repeated at least three times with 15 oocytes per group. EtOH, ethanol.

(Fig. 1D), we still observed perturbed AURKC-CPC ICA localization and activity (supplementary material Fig. S4A–C). We note that kinetochore signals were slightly lower, although not absent, compared with those of controls. Because chromosome morphology is grossly altered in haspin-overexpressing oocytes, we do not know whether AURKC-CPC localization is also sensitive to high levels of H3pT3 or if the elongated morphology makes the localization appear diffuse by our detection methods. Furthermore, we observed a partial rescue in AURKC ICA localization when wild-type but not catalytically inactive haspin was overexpressed in 5-Itu-treated oocytes (supplementary material Fig. S4D). That is, within the same oocytes, some chromosomes displayed more clear AURKC ICA localization than others. These data might reflect the need for a

precise amount of H3pT3 that we cannot control in our experimental procedure.

Inhibition of haspin perturbs kinetochore–microtubule attachments causing aneuploidy

AURKC is required to regulate chromosome alignment during Met I through destabilizing improper kinetochore–microtubule attachments (Balboula and Schindler, 2014). When AURKC activity is inhibited, oocytes that mature to Met II are aneuploid. To determine whether altered AURKC-CPC arm localization is associated with these meiotic defects, we first matured oocytes in the presence of 5-Itu to Met I to assess chromosome alignment in the oocytes that had a bipolar spindle. We found that as the dose of 5-Itu increased, the percentage of chromosome misalignment also increased. 18.56%±3.68% (mean±s.e.m.) of control oocytes had chromosomes not properly aligned on the Met I plate and 27.78%±10% of oocytes incubated in 100 nM 5-Itu had chromosome misalignment (data not shown). Oocytes incubated in 500 nM 5-Itu had a significant increase in chromosome misalignment ($P<0.05$, one-way ANOVA), as 49.78%±7.95% were aberrant (data not shown). Therefore, inhibition of haspin causes chromosome misalignment at the Met I plate.

Next, we performed an assay to assess the types of attachments the spindle made to kinetochores. Spindle fibers attached to kinetochores are stable under conditions such as cold treatment, whereas the remainder of the spindle is sensitive and depolymerizes (Rieder, 1981). This treatment allows better visualization of the kinetochore-attached microtubules. After a brief pulse of cold medium, we fixed oocytes and performed immunocytochemistry to detect the attached microtubules and kinetochores. We found that when incubated in 500 nM of 5-Itu, 30% of kinetochores displayed abnormal attachments (fibers that did not come from one pole to attach to both sister kinetochores) and 30% were not attached at all (Fig. 6A,B). Less than 10% of controls contained these defects. Similarly, when we assessed attachments in oocytes overexpressing haspin compared with *Gfp*-injected controls, nearly 55% of kinetochores were improperly attached (Fig. 6C,D).

Finally, to assess the consequences of these defects, we matured oocytes to Met II and performed an *in situ* chromosome spread to determine chromosome number. The data showed that when haspin was inhibited or overexpressed, ~60% of oocytes were aneuploid (Fig. 6E,F). However, the chromosome morphology at Met II and types of aneuploidy were different between the experimental groups. When we inhibited haspin, the chromosome morphology at Met II was more rounded (Fig. 3C), and the eggs typically contained one extra or one fewer univalent. By contrast, the chromosomes in eggs containing excess haspin were hypercondensed (Fig. 3C), and we frequently observed separated sister chromatids even when the chromosome count was normal (totaling 40) (Fig. 3C; Fig 6F). Furthermore, the chromosome content ranged from 36 to 42, indicating that MI was severely aberrant, consistent with the presence of chromosome bridges in Ana I (Fig. 1C). The presence of separated sisters at Met II but presence of REC8 and SGO2L at Met I indicates that either cohesin is not being protected after Met I or that the rigidity of the chromosomes is somehow causing the sisters to fall apart once the spindle begins to pull during Ana I. In summary, perturbing AURKC localization at the ICA by either haspin inhibition or overexpression alters the ability of the oocytes to correct improper kinetochore–microtubule attachments, leading to misalignment at the Met I plate and, ultimately, to aneuploidy in Met II eggs. Because these phenotypes are similar to that of global inhibition of AURKC (Balboula and Schindler, 2014), the data suggest that ICA-localized AURKC-CPC, and not kinetochore-localized AURKC-CPC, regulate the attachment process during MI.

DISCUSSION

Although haspin was originally identified as a haploid-cell-specific gene (Tanaka et al., 1999), its function in meiosis or in oocytes was not yet determined. This is the first report to confirm that mouse oocytes contain active haspin kinase and to define a role for its function. We find that its activity is required for several steps of MI. First, haspin is required to promote meiotic resumption (Fig. 2C), and later, haspin regulates the localization of AURKC-CPC to the ICA (Fig. 5). Similar to loss of AURKC function (Balboula and Schindler, 2014), when oocytes have perturbed haspin activity, there is a persistence of improper kinetochore–microtubule attachments that ultimately leads to aneuploid eggs (Fig. 6). Therefore, haspin is a crucial regulator of MI chromosome segregation in mouse oocytes.

It is intriguing that haspin mRNA is much more highly expressed in meiotic cells compared with mitotic cells (Tanaka et al., 1999). Because MI involves keeping sister chromatids together while homologs segregate, it is possible that haspin plays additional or different roles in regulating MI than it does in regulating mitotic chromosome segregation. Our findings that H3T3 phosphorylation extends along the ICA at Met I (Fig. 1A), where other meiosis-specific proteins localize (Balboula and Schindler, 2014; Lee et al., 2008; Shuda et al., 2009) are consistent with this hypothesis. AURKC is also more highly expressed in meiotic cells and has a MI-specific localization at the ICA (Balboula and Schindler, 2014; Schindler et al., 2012; Shuda et al., 2009). In mitosis, phosphorylation of H3T3 at centromeres drives AURKB localization to this locale, where it is required to regulate kinetochore–microtubule attachments (Dai et al., 2006; Markaki et al., 2009; Wang et al., 2010; Wang et al., 2012; Wang et al., 2011; Yamagishi et al., 2010). We found that inhibition of haspin specifically affects the localization of AURKC at the ICA, and not at the kinetochore (Fig. 5). However, improper kinetochore–microtubule attachments persist following haspin inhibition (Fig. 6A). These data suggest that, unlike in mitosis, ICA-localized AURKC-CPC regulates these attachments. Consistent with this hypothesis is recent data demonstrating that kinetochore-localized AURKC is not activated at Met I (Rattani et al., 2013). Therefore, our data provide insight into the importance of localized AURKC-CPC activity at chromosome arms and how that targeting is controlled. Furthermore, these data suggest that meiosis-specific signaling molecules modify mitotic chromosome segregation to meet the needs of MI.

In contrast to a report on the role of haspin in mitosis (Dai et al., 2006), we found that sister chromatid cohesion appeared to be intact but chromosome condensation was perturbed (Figs 3, 4). Condensins play an essential role in establishing chromosome architecture and regulating chromosome segregation (Hirano, 2012; Kimura et al., 2001; Losada et al., 2002; Ono et al., 2003). SMC2, the subunit common to both condensin I and II fails to localize to chromosomes when haspin is inhibited, and twice as much localizes when haspin is overexpressed (Fig. 3). The chromosome morphology phenotypes that we observed following haspin inhibition and overexpression are consistent with the reported phenotypes associated with loss and gain of condensin

Journal of Cell Science (2014) 127, 5066–5078 doi:10.1242/jcs.158840

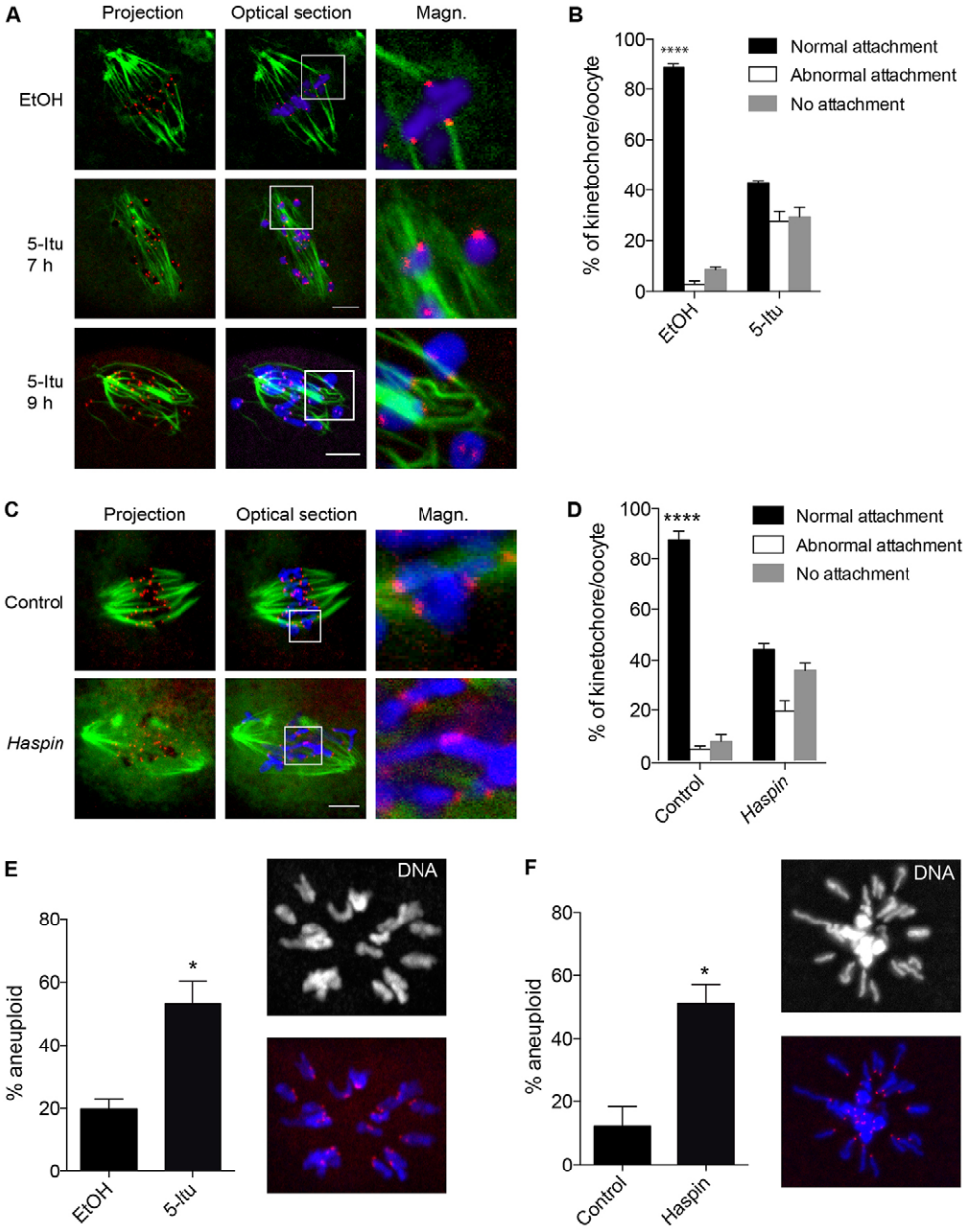

Fig. 6. Perturbation of haspin alters kinetochore–microtubule attachments and causes aneuploidy. (A,B) Prophase-I-arrested oocytes were isolated and matured *in vitro* to Met I (7 h and 9 h) in the presence of 500 nM 5-Itu prior to exposure to cold medium and fixation. Microtubules (green), kinetochores (red) and DNA (blue) were detected by confocal microscopy. Shown are representative *Z*-projections and optical slices. (B) Quantification of the types of attachments of each kinetochore per oocyte. At least 12 kinetochores were analyzed per oocyte and 40 oocytes were analyzed per group. (C,D) Prophase-I-arrested oocytes were isolated, microinjected with buffer or haspin cRNA and matured *in vitro* to Met I (7 h) prior to exposure to cold medium and fixation. Analysis was conducted as in A,B. Magn., magnified view of the area outlined in white. Scale bars: 10 µm. (E) Germinal-vesicle-intact oocytes were isolated and matured *in vitro* to Met II (16 h) in the presence of 500 nM 5-Itu. (F) Oocytes were treated as in E, but were microinjected with buffer or haspin cRNA prior to maturation. For E,F, after maturation, eggs were exposed to monastrol to collapse the spindle and spread the chromosomes. After fixation, DNA (blue in merge) and kinetochores (red in merge) were detected by epifluorescence microscopy. The images on the right demonstrate a typical spread and the difference in chromosome morphology between 5-Itu and overexpression treatments. All experiments were repeated three times. The quantitative data show the mean±s.e.m.; $*P<0.05$; $****P<0.0001$ [Student's *t*-test (F,G), two-way ANOVA (B,D)]. EtOH, ethanol.

II, respectively (Lee et al., 2011). These phenotypes include controlling bivalent individualization, compaction and resolution prior to loss of cohesin during anaphase onset, and chromosome misalignment. Interestingly, the spatiotemporal dynamics of the complexes differ between mitosis and meiosis (Lee et al., 2011). In mitosis, condensin I loads onto chromosomes in prometaphase, whereas in oocyte meiosis it is restricted at centromeres through Met I and does not associate with chromosomes until Ana I. Condensin II loads onto chromosome axes prior to NEBD in mitosis, but loads after NEBD during meiosis. Therefore, compared with mitosis, there is a delay in condensin loading in meiosis. We found an increase in H3T3 phosphorylation after NEBD (supplementary material Fig. S1). In other systems, AURKB regulates the localization of condensin I (Bembenek et al., 2013; Collette et al., 2011; Lipp et al., 2007; Nakazawa et al., 2011). Given that inhibition of haspin prevents AURKC-CPC from localizing to chromosomes, it is feasible that the loss of SMC2 localization is a direct consequence of loss of localized AURKC-CPC activity. However, we cannot at this point rule out a direct effect of loss of H3pT3 on condensin loading. Moreover, because we observe loss of SMC2 on chromosomes in Met I (Fig. 3), it is likely that haspin inhibition is preventing condensin II loading. The differences of condensin and Aurora-CPC localizations and functions between mitosis and meiosis are intriguing and future studies will shed light on how these complexes control MI to prevent aneuploidy.

Mammalian oocytes contain both AURKB and AURKC, which are highly similar in sequence and in biochemical function (Fernández-Miranda et al., 2011; Sasai et al., 2004; Schindler et al., 2012; Slattery et al., 2009). In mitosis, phosphorylation of H3T3 by haspin drives AURKB-CPC to kinetochores (Wang et al., 2010; Wang et al., 2011; Yamagishi et al., 2010). However, in meiosis, AURKC localizes to kinetochores and the ICA, whereas AURKB localizes to the spindle (Balboula and Schindler, 2014). We previously showed that although AURKB can compensate for AURKC in *Aurkc*$^{-/-}$ oocytes, AURKC has

non-overlapping functions from AURKB in wild-type oocytes (Balboula and Schindler, 2014; Schindler et al., 2012). These functions include regulating the correction of improper kinetochore–microtubule attachments to ensure correct chromosome alignment and segregation during MI (Balboula and Schindler, 2014). Because haspin and H3pT3 have a similar localization pattern to AURKC, haspin inhibition delocalizes ICA-localized AURKC, and these oocytes have similar phenotypes to those of oocytes with loss of AURKC activity, we attribute the defects to loss of localized AURKC-CPC function (Balboula and Schindler, 2014). We do not yet know formally whether haspin has a meiosis-specific role in regulating AURKB. Furthermore, we detected haspin at the polarized actin cap in Met II eggs (Fig. 1E). In budding yeast, the haspin homologs, Alk1 and Alk2 regulate actin distribution to coordinate cell polarization with the cell cycle (Panigada et al., 2013). Therefore, further studies are warranted to determine the specificity of haspin for the AURKs and potential roles in regulating egg or embryonic polarity.

Our studies reveal that regulation of AURKC-CPC localization is complex (Balboula and Schindler, 2014; Balboula et al., 2014). Histone modifications appear to be the main driving force of regulation. For instance, AURKC-CPC is lost from kinetochores and the ICA in oocytes depleted for RBBP7, a component of histone deacetylase complexes. In these oocytes, histones are hyperacetylated and display the hallmark phenotypes associated with loss of AURKC activity – chromosome misalignment, a persistence of improper kinetochore–microtubule attachments and aneuploidy. In this case, overexpression of AURKC can rescue the localization and phenotypic defects. Therefore, histone acetylation might be required to maintain AURKC localization. By contrast, phosphorylation of H3T3 by haspin appears to regulate AURKC-CPC loading because overexpression does not restore its ICA localization or rescue the phenotypic defects. Most intriguing is the specificity for regulating the loading of a subpopulation AURKC. In mitosis, BUB1 phosphorylates histone H2A at T120 at centromeres, and also participates in regulating AURKB-CPC localization (Yamagishi et al., 2010). It will be of interest to investigate this regulatory pathway in oocyte meiosis to determine whether there is specificity for regulating the kinetochore population of AURKC. In summary, these studies are the first to shed light on localized AURKC function and to highlight important differences in how chromosome segregation is regulated between MI and mitosis.

MATERIALS AND METHODS

cDNA synthesis and RT-PCR

A total of 50 oocytes or embryos at the indicated stages were isolated from CF-1 mice and frozen before processing. *Gfp* mRNA (2 ng) was added to each sample and total RNA from the mixtures was purified using the PicoPure RNA isolation kit (Life Technologies, Grand Island, NY) according to the manufacturer's protocol. Using random hexamers and SuperScript II, cDNA was generated by reverse transcription. Taqman probes specific for haspin (Mm00494767_s1) (Life Technologies, Grand Island, NY) were used for gene expression detection and the comparative C_t method was used to determine the difference in expression levels between stages. Data were acquired using an ABI Prism 7000 (Life Technologies, Grand Island, NY).

Oocyte collection, microinjection and maturation

Sexually mature CF-1 mice (6–8 weeks, Harlan Laboratories, Indianapolis, IN) were hormonally primed by an intraperitoneal injection of 5 IU of equine gonadotropin (EMD Millipore, Billerica, MA). Germinal-vesicle-intact oocytes were isolated from antral follicles at 44–46 h after injection, in MEM/PVP (polyvinylpyrrolidone) containing 2.5 µM milrinone (Sigma, St Louis, MO; #M4659) to prevent meiotic maturation (Tsafriri et al., 1996). All oocytes were matured at 37℃ in a humidified atmosphere of 5% CO_2 in Chatot, Ziomek, Bavister (CZB) medium. Oocytes were microinjected with 7–10 pl of the indicated cRNA. Injections were performed in MEM plus 2.5 µM milrinone using a Xenoworks digital microinjector (Sutter Instruments, Novato, CA). All animal experiments were approved by the institutional animal use and care committee and were consistent with NIH guidelines.

Haspin inhibition

Oocytes were incubated in the presence of 5-iodotubercidin (5-Itu) (Cayman Chemical, Ann Arbor, MI; #10010375) or CHR-6494 (CHR) (a gift from Chroma Therapeutics, Abingdon, Oxon, UK) diluted in CZB (1:1000 and 1:2000, respectively). 100% ethanol (1:1000) was used as a control in all 5-Itu experiments and DMSO (1:2000) was used as a control in all CHR experiments. For the rescue experiments, oocytes were incubated in 5-Itu for 1 h prior to microinjection, recovery and maturation in 5-Itu. *In vitro* maturation occurred in organ culture dishes that were kept humid with a surrounding water chamber to avoid the partitioning of the drugs into an oil overlay.

Cloning and *in vitro* synthesis of cRNA

To generate GFP-tagged haspin and *Sgol2*, cDNAs were PCR-amplified from commercially available clones (GE Healthcare, Little Chalfont, Buckinghamshire, UK; clone IDs 40054435 and 6833875, respectively), ligated into pIVT-*Gfp* (Igarashi et al., 2007) and confirmed by sequencing. Haspin was tagged with GFP at the N-terminus and SGOL2 at the C-terminus. K466 (5′-AAA-3′) of haspin was mutated to an R (5′-AGA-3′) using the QuikChange Lightning Multi Site-Directed Mutagenesis kit (Agilent Technologies, Santa Clara, CA). After DNA linearization with *Nde*I and purification, cRNA was generated *in vitro* using an mMessage mMachine T7 kit (Life Technologies, Grand Island, NY). The final product was purified using an RNeasy kit (Qiagen, Veno, Limburg, The Netherlands). Haspin cRNA was injected at 600 ng/µl and *Sgol2* cRNA at 500 ng/µl.

Immunocytochemistry

For AURKC, H3pT3 and pINCENP detection, oocytes were fixed using 2% paraformaldehyde (PFA) in phosphate-buffered saline (PBS) for 20 min followed by permeabilization (PBS, 0.1% v/v Triton X-100, 0.3% w/v BSA) for 20 min. The oocytes were then incubated in appropriate antibodies diluted in blocking solution (PBS, 0.3% w/v BSA, 0.01% v/v Tween-20) for 1 h in a humidified chamber. After incubation in primary antibody solution, cells were washed and incubated for an additional hour in similarly diluted secondary antibody in a humidified chamber. Cells were mounted in 5 µl of Vectashield (Vector Laboratories, Burlingame, CA) containing DAPI (1:333, Sigma, St Louis, MO). For detection of REC8 and survivin, cells were fixed using 2% PFA in PBS+0.1% Triton X-100 (Sigma, St Louis, MO) for 20 min or 4% PFA in PBS at 4℃ overnight, respectively. Permeabilization, staining and mounting were performed according to above parameters. SMC2 detection (1:1000) (gift from Tatsuya Hirano, RIKEN, Japan), *in situ* ploidy, chromosome spreads and cold-stable microtubule assays were performed as described previously (Balboula and Schindler, 2014; Duncan et al., 2009; Lampson and Kapoor, 2005; Lee et al., 2011; Stein and Schindler, 2011; Chiang et al., 2010).

The following antibodies were used for immunofluorescence: anti-AURKC (Bethyl Laboratories, Montgomery, TX; #A300-BL1217) at 1:30, CREST (Antibodies Inc., Davis, CA; #15-234) at 1:100, anti-H3pT3 (Active Motif, Carlsbad, CA; #39153) at 1:100, anti-pINCENP (a gift from Michael Lampson, University of Pennsylvania, PA) at 1:500, anti-REC8 (a gift from Richard Schultz, University of Pennsylvania, PA) at 1:1000, anti-survivin (Cell Signaling Technology, Beverly, MA; #2808S) at 1:500, anti-SMC2 at 1:1000, anti-α-tubulin conjugated to Alexa Fluor 488 (Cell Signaling Technology, Beverly, MA; #5063S or Life Technologies, Grand Island, NY; #322588) at 1:100. The following

secondary antibodies were from Life Technologies (Grand Island, NY) and used at a 1:200 dilution: Alexa-Fluor-488-conjugated goat anti-mouse-IgG (#A10680), Alexa-Fluor-546-conjugated rabbit anti-mouse-IgG (#A11060), Alexa-Fluor-546-conjugated donkey anti-rabbit-IgG (#A10040) and Alexa-Fluor-633-conjugated goat anti-human-IgG (#A21091). The actin cap was detected by adding 2 drops/ml of Actin Red 555 Ready Probes reagent (Life Technologies, Grand Island, NY; #R37112) to eggs in blocking solution that were previously fixed and permeabilized for 30 min. To depolymerize the actin cap, eggs were treated with 10 µM latrunculin A (Cayman Chemical, Ann Arbor, MI; #10010630) for 10 min prior to fixation.

Imaging

A Zeiss 510 Meta laser-scanning confocal microscope with a 40× or 63× objective was used for imaging. Optical *Z* slices were obtained using 1.0–1.5-µm steps with a zoom of 2. When signal intensities were compared, laser power was kept constant for each oocyte in an experiment. For ploidy analyses, images were obtained using Zeiss Axiovert 200M epifluorescence microscope with a 63× objective. For live-cell imaging, oocytes were placed into a glass-bottomed 96-well dish (Greiner Bio One, Monroe, NC) and images were acquired using an EVOS FL Auto Imaging System (Life Technologies, Grand Island, NY) with a 20× objective. The microscope stage was heated to 37˚C and 5% CO_2 was maintained.

Image analysis

All images were processed and analyzed using ImageJ (NIH, Bethesda, MD). Prior to analysis, individual *Z* slices were first overlaid and the final *Z*-projection image was used for analysis. Pixel intensities were determined by subtracting an average background intensity signal from an average pixel signal restricted to chromosomes or a selected region of the chromosome. Chromosome alignment was scored according to the parameters described by Lane and colleagues (Lane et al., 2012). Only oocytes exhibiting bipolar spindles were used for alignment analysis. Chromosome morphology (Fig. 3A) was qualitatively scored according to the following parameters: ‘normal’ if bivalents were distinguishable, ‘rounded’ if they exhibited short and dense chromosomes without distinguishable bivalents, and ‘extended’ if they had a distinctive pointy appearance. To assess the localization of CPC-associated proteins AURKC, survivin and pINCENP, Met I oocytes were characterized as having one of three phenotypes: ‘kinetochore plus axis distribution’, in which a clear localization at the kinetochores and along the ICA was visible; ‘kinetochore plus diffuse ICA localization’, where no clear line at the ICA was present; and ‘diffuse DNA staining’, with no clear kinetochore or ICA localization. Qualitative assessments were confirmed using the ‘plot profiles’ function in ImageJ to measure pixel intensity along the chromatid axes from kinetochore to kinetochore.

Statistical analyses

Statistical significance was calculated using Prism Graphpad Software (La Jolla, CA). *P*-values were obtained using Student’s *t*-test or one-way or two-way ANOVA, as indicated in the legends, with Tukey post-tests and 0.05% confidence intervals.

Acknowledgements

The authors acknowledge Brianna Fram (University of Pennsylvania, Philadelphia, PA) for assistance with the RT-PCR and H3pT3 immunofluorescence, Catalina Munoz (Rutgers University, Piscataway, NJ) for assisting with the NEBD studies, Michael Lampson for the pINCENP antibody, Richard Schultz for the REC8 antibody, Tatsuya Hirano for the SMC2 antibody and Chroma Therapeutics for CHR-6494. We also thank Jessica Fellmeth (Rutgers University, Piscataway, NJ) for feedback.

Competing interests

The authors declare no competing interests.

Author contributions

A.L.N., A.S.G., A.Z.B., V.S. and J.O. performed and analyzed experiments. K.S. designed and performed experiments and wrote the manuscript. All co-authors corrected the manuscript.

Funding

This work was supported by funding from the National Institutes of Health [grant number R00HD061657]; and Rutgers University institutional start-up funds. Deposited in PMC for release after 12 months.

Supplementary material

Supplementary material available online at
http://jcs.biologists.org/lookup/suppl/doi:10.1242/jcs.158840/-/DC1

References

Ashtiyani, R. K., Moghaddam, A. M., Schubert, V., Rutten, T., Fuchs, J., Demidov, D., Blattner, F. R. and Houben, A. (2011). AtHaspin phosphorylates histone H3 at threonine 3 during mitosis and contributes to embryonic patterning in Arabidopsis. *Plant J.* **68**, 443-454.

Balboula, A. Z. and Schindler, K. (2014). Selective disruption of aurora C kinase reveals distinct functions from aurora B kinase during meiosis in mouse oocytes. *PLoS Genet.* **10**, e1004194.

Balboula, A. Z., Stein, P., Schultz, R. M. and Schindler, K. (2014). Knockdown of RBBP7 unveils a requirement of histone deacetylation for CPC function in mouse oocytes. *Cell Cycle* **13**, 600-611.

Bembenek, J. N., Verbrugghe, K. J., Khanikar, J., Csankovszki, G. and Chan, R. C. (2013). Condensin and the spindle midzone prevent cytokinesis failure induced by chromatin bridges in C. elegans embryos. *Curr. Biol.* **23**, 937-946.

Carmena, M., Wheelock, M., Funabiki, H. and Earnshaw, W. C. (2012). The chromosomal passenger complex (CPC): from easy rider to the godfather of mitosis. *Nat. Rev. Mol. Cell Biol.* **13**, 789-803.

Chiang, T., Duncan, F. E., Schindler, K., Schultz, R. M. and Lampson, M. A. (2010). Evidence that weakened centromere cohesion is a leading cause of age-related aneuploidy in oocytes. *Curr. Biol.* **20**, 1522-1528.

Collette, K. S., Petty, E. L., Golenberg, N., Bembenek, J. N. and Csankovszki, G. (2011). Different roles for Aurora B in condensin targeting during mitosis and meiosis. *J. Cell Sci.* **124**, 3684-3694.

Dai, J. and Higgins, J. M. (2005). Haspin: a mitotic histone kinase required for metaphase chromosome alignment. *Cell Cycle* **4**, 665-668.

Dai, J., Sultan, S., Taylor, S. S. and Higgins, J. M. (2005). The kinase haspin is required for mitotic histone H3 Thr 3 phosphorylation and normal metaphase chromosome alignment. *Genes Dev.* **19**, 472-488.

Dai, J., Sullivan, B. A. and Higgins, J. M. (2006). Regulation of mitotic chromosome cohesion by Haspin and Aurora B. *Dev. Cell* **11**, 741-750.

Dai, J., Kateneva, A. V. and Higgins, J. M. (2009). Studies of haspin-depleted cells reveal that spindle-pole integrity in mitosis requires chromosome cohesion. *J. Cell Sci.* **122**, 4168-4176.

De Antoni, A., Maffini, S., Knapp, S., Musacchio, A. and Santaguida, S. (2012). A small-molecule inhibitor of Haspin alters the kinetochore functions of Aurora B. *J. Cell Biol.* **199**, 269-284.

Duncan, F. E., Chiang, T., Schultz, R. M. and Lampson, M. A. (2009). Evidence that a defective spindle assembly checkpoint is not the primary cause of maternal age-associated aneuploidy in mouse eggs. *Biol. Reprod.* **81**, 768-776.

Fernández-Miranda, G., Trakala, M., Martín, J., Escobar, B., González, A., Ghyselinck, N. B., Ortega, S., Cañamero, M., Pérez de Castro, I. and Malumbres, M. (2011). Genetic disruption of aurora B uncovers an essential role for aurora C during early mammalian development. *Development* **138**, 2661-2672.

Higgins, J. M. (2003). Structure, function and evolution of haspin and haspin-related proteins, a distinctive group of eukaryotic protein kinases. *Cell. Mol. Life Sci.* **60**, 446-462.

Hirano, T. (2012). Chromosome territories meet a condensin. *PLoS Genet.* **8**, e1002939.

Huertas, D., Soler, M., Moreto, J., Villanueva, A., Martinez, A., Vidal, A., Charlton, M., Moffat, D., Patel, S., McDermott, J. et al. (2012). Antitumor activity of a small-molecule inhibitor of the histone kinase Haspin. *Oncogene* **31**, 1408-1418.

Hunt, P. A. and Hassold, T. J. (2002). Sex matters in meiosis. *Science* **296**, 2181-2183.

Igarashi, H., Knott, J. G., Schultz, R. M. and Williams, C. J. (2007). Alterations of PLCbeta1 in mouse eggs change calcium oscillatory behavior following fertilization. *Dev. Biol.* **312**, 321-330.

Kelly, A. E. and Funabiki, H. (2009). Correcting aberrant kinetochore microtubule attachments: an Aurora B-centric view. *Curr. Opin. Cell Biol.* **21**, 51-58.

Kelly, A. E., Ghenoiu, C., Xue, J. Z., Zierhut, C., Kimura, H. and Funabiki, H. (2010). Survivin reads phosphorylated histone H3 threonine 3 to activate the mitotic kinase Aurora B. *Science* **330**, 235-239.

Kimura, K., Cuvier, O. and Hirano, T. (2001). Chromosome condensation by a human condensin complex in Xenopus egg extracts. *J. Biol. Chem.* **276**, 5417-5420.

Lampson, M. A. and Kapoor, T. M. (2005). The human mitotic checkpoint protein BubR1 regulates chromosome-spindle attachments. *Nat. Cell Biol.* **7**, 93-98.

Lane, S. I., Yun, Y. and Jones, K. T. (2012). Timing of anaphase-promoting complex activation in mouse oocytes is predicted by microtubule-kinetochore attachment but not by bivalent alignment or tension. *Development* **139**, 1947-1955.

Lee, J., Kitajima, T. S., Tanno, Y., Yoshida, K., Morita, T., Miyano, T., Miyake, M. and Watanabe, Y. (2008). Unified mode of centromeric protection by shugoshin in mammalian oocytes and somatic cells. *Nat. Cell Biol.* **10**, 42-52.

Lee, J., Ogushi, S., Saitou, M. and Hirano, T. (2011). Condensins I and II are essential for construction of bivalent chromosomes in mouse oocytes. *Mol. Biol. Cell* **22**, 3465-3477.
Li, X., Sakashita, G., Matsuzaki, H., Sugimoto, K., Kimura, K., Hanaoka, F., Taniguchi, H., Furukawa, K. and Urano, T. (2004). Direct association with inner centromere protein (INCENP) activates the novel chromosomal passenger protein, Aurora-C. *J. Biol. Chem.* **279**, 47201-47211.
Lipp, J. J., Hirota, T., Poser, I. and Peters, J. M. (2007). Aurora B controls the association of condensin I but not condensin II with mitotic chromosomes. *J. Cell Sci.* **120**, 1245-1255.
Losada, A., Hirano, M. and Hirano, T. (2002). Cohesin release is required for sister chromatid resolution, but not for condensin-mediated compaction, at the onset of mitosis. *Genes Dev.* **16**, 3004-3016.
Maiolica, A., de Medina-Redondo, M., Schoof, E. M., Chaikuad, A., Villa, F., Gatti, M., Jeganathan, S., Lou, H. J., Novy, K., Hauri, S. et al. (2014). Modulation of the chromatin phosphoproteome by the Haspin protein kinase. *Mol. Cell. Proteomics* **13**, 1724-1740.
Markaki, Y., Christogianni, A., Politou, A. S. and Georgatos, S. D. (2009). Phosphorylation of histone H3 at Thr3 is part of a combinatorial pattern that marks and configures mitotic chromatin. *J. Cell Sci.* **122**, 2809-2819.
Nakazawa, N., Mehrotra, R., Ebe, M. and Yanagida, M. (2011). Condensin phosphorylated by the Aurora-B-like kinase Ark1 is continuously required until telophase in a mode distinct from Top2. *J. Cell Sci.* **124**, 1795-1807.
Niedzialkowska, E., Wang, F., Porebski, P. J., Minor, W., Higgins, J. M. and Stukenberg, P. T. (2012). Molecular basis for phosphospecific recognition of histone H3 tails by Survivin paralogues at inner centromeres. *Mol. Biol. Cell* **23**, 1457-1466.
Ono, T., Losada, A., Hirano, M., Myers, M. P., Neuwald, A. F. and Hirano, T. (2003). Differential contributions of condensin I and condensin II to mitotic chromosome architecture in vertebrate cells. *Cell* **115**, 109-121.
Panigada, D., Grianti, P., Nespoli, A., Rotondo, G., Castro, D. G., Quadri, R., Piatti, S., Plevani, P. and Muzi-Falconi, M. (2013). Yeast haspin kinase regulates polarity cues necessary for mitotic spindle positioning and is required to tolerate mitotic arrest. *Dev. Cell* **26**, 483-495.
Qian, J., Lesage, B., Beullens, M., Van Eynde, A. and Bollen, M. (2011). PP1/Repo-man dephosphorylates mitotic histone H3 at T3 and regulates chromosomal aurora B targeting. *Curr. Biol.* **21**, 766-773.
Rattani, A., Wolna, M., Ploquin, M., Helmhart, W., Morrone, S., Mayer, B., Godwin, J., Xu, W., Stemmann, O., Pendas, A. et al. (2013). Sgol2 provides a regulatory platform that coordinates essential cell cycle processes during meiosis I in oocytes. *eLife* **2**, e01133.
Rieder, C. L. (1981). The structure of the cold-stable kinetochore fiber in metaphase PtK1 cells. *Chromosoma* **84**, 145-158.
Sasai, K., Katayama, H., Stenoien, D. L., Fujii, S., Honda, R., Kimura, M., Okano, Y., Tatsuka, M., Suzuki, F., Nigg, E. A. et al. (2004). Aurora-C kinase is a novel chromosomal passenger protein that can complement Aurora-B kinase function in mitotic cells. *Cell Motil. Cytoskeleton* **59**, 249-263.
Schindler, K., Davydenko, O., Fram, B., Lampson, M. A. and Schultz, R. M. (2012). Maternally recruited Aurora C kinase is more stable than Aurora B to support mouse oocyte maturation and early development. *Proc. Natl. Acad. Sci. U. S. A.* **109**, E2215-E2222.
Sharif, B., Na, J., Lykke-Hartmann, K., McLaughlin, S. H., Laue, E., Glover, D. M. and Zernicka-Goetz, M. (2010). The chromosome passenger complex is required for fidelity of chromosome transmission and cytokinesis in meiosis of mouse oocytes. *J. Cell Sci.* **123**, 4292-4300.
Shuda, K., Schindler, K., Ma, J., Schultz, R. M. and Donovan, P. J. (2009). Aurora kinase B modulates chromosome alignment in mouse oocytes. *Mol. Reprod. Dev.* **76**, 1094-1105.
Slattery, S. D., Mancini, M. A., Brinkley, B. R. and Hall, R. M. (2009). Aurora-C kinase supports mitotic progression in the absence of Aurora-B. *Cell Cycle* **8**, 2986-2997.
Stein, P. and Schindler, K. (2011). Mouse oocyte microinjection, maturation and ploidy assessment. *J. Vis. Exp.* **53**, 2851.
Tanaka, H., Yoshimura, Y., Nozaki, M., Yomogida, K., Tsuchida, J., Tosaka, Y., Habu, T., Nakanishi, T., Okada, M., Nojima, H. et al. (1999). Identification and characterization of a haploid germ cell-specific nuclear protein kinase (Haspin) in spermatid nuclei and its effects on somatic cells. *J. Biol. Chem.* **274**, 17049-17057.
Tsafriri, A., Chun, S. Y., Zhang, R., Hsueh, A. J. and Conti, M. (1996). Oocyte maturation involves compartmentalization and opposing changes of cAMP levels in follicular somatic and germ cells: studies using selective phosphodiesterase inhibitors. *Dev. Biol.* **178**, 393-402.
Tseng, T. C., Chen, S. H., Hsu, Y. P. and Tang, T. K. (1998). Protein kinase profile of sperm and eggs: cloning and characterization of two novel testis-specific protein kinases (AIE1, AIE2) related to yeast and fly chromosome segregation regulators. *DNA Cell Biol.* **17**, 823-833.
Wang, F., Dai, J., Daum, J. R., Niedzialkowska, E., Banerjee, B., Stukenberg, P. T., Gorbsky, G. J. and Higgins, J. M. (2010). Histone H3 Thr-3 phosphorylation by Haspin positions Aurora B at centromeres in mitosis. *Science* **330**, 231-235.
Wang, F., Ulyanova, N. P., van der Waal, M. S., Patnaik, D., Lens, S. M. and Higgins, J. M. (2011). A positive feedback loop involving Haspin and Aurora B promotes CPC accumulation at centromeres in mitosis. *Curr. Biol.* **21**, 1061-1069.
Wang, F., Ulyanova, N. P., Daum, J. R., Patnaik, D., Kateneva, A. V., Gorbsky, G. J. and Higgins, J. M. (2012). Haspin inhibitors reveal centromeric functions of Aurora B in chromosome segregation. *J. Cell Biol.* **199**, 251-268.
Yamagishi, Y., Honda, T., Tanno, Y. and Watanabe, Y. (2010). Two histone marks establish the inner centromere and chromosome bi-orientation. *Science* **330**, 239-243.